Available online at www.sciencedirect.com
SCIENCE DIRECT®
International Journal of Heat and Mass Transfer 47 (2004) 4089–4099
International Journal of HEAT and MASS TRANSFER
www.elsevier.com/locate/ijhmt

Liquid-mixed convection in a closed enclosure with highly-intensive heat fluxes

A. Rivas-Cardona [a], A. Hernandez-Guerrero [a,*], R. Romero-Méndez [b], R. Lesso-Arroyo [c]

[a] Facultad de Ingeniería Mecánica, Eléctrica y Electrónica, Universidad de Guanajuato, Tampico 912, Col. Bellavista, C.P. 36730, Salamanca, Guanajuato, Mexico

[b] Facultad de Ingeniería, Universidad Autónoma de San Luis Potosí, Av. Dr. Manuel Nava 8, Zona Universitaria, C.P. 78290, San Luis Potosí, SLP, Mexico

[c] Instituto Tecnológico de Celaya, Departamento de Ingeniería Mecánica, Avenida Tecnológico S/N, Celaya Gto., Mexico

Received 19 February 2004; received in revised form 12 May 2004

Abstract

Laminar-mixed convection of a dielectric fluid contained in a two-dimensional enclosure is investigated in the present paper. Within the enclosure discrete heat sources of a constant heat flux are flush-mounted on a vertical wall. Forced flow conditions are imposed by placing a propeller at different locations within the enclosure. The analysis is performed for a wide range of heat fluxes, from the order of 10,000 to 100,000 W/m^2, way in the trend of current computer chips, such as the Pentium IV, and the future ones. Emphasis is placed on the influence of the governing parameters, such as buoyancy parameters, the aspect ratio of the enclosure, and location of the propeller. The flow and temperature fields are obtained as part of the solution.
© 2004 Elsevier Ltd. All rights reserved.

Keywords: Energy dissipation; Dielectric fluid; Large heat fluxes; Mixed convection; Enclosure

1. Introduction

Since the development of the first electronic computers in the 1940s, the demand for faster and denser circuit technologies and packages has been accompanied by increasing heat fluxes at the chip and package levels. Based on the extrapolation of historical trends, microprocessor power is expected to reach 200 W within a few years with the average power density reaching values as high as 125 W/cm^2 [1]. Over the years, significant advances have been made in the application of air cooling techniques, involving either free or forced convection, to dissipate the energy coming out of the computer chips.

Several analyses have been carried out to investigate the parameters that affect the convective heat transfer in an enclosure with heat sources mounted on its walls. Sezai and Mohamad [2] numerically studied the three-dimensional effect of free convection in a rectangular enclosure. A heat source was placed on the bottom of the enclosure. Two cases were analyzed: one in which vertical walls were considered as adiabatic and a second one with the vertical walls maintained at a constant temperature. The aspect ratio was varied for both cases. At Rayleigh numbers of the order of 10^3, energy from the heat source was mainly dissipated by conduction, while at $Ra > 10^3$ heat transfer was dominated by the advection mechanism. Deng et al. [3] numerically investigated steady natural convection induced by multiple discrete heat sources in two-dimensional horizontal

* Corresponding author. Tel.: +52-464-80911x221; fax: +52-464-72400.
E-mail address: abelh@salamanca.ugto.mx (A. Hernandez-Guerrero).

0017-9310/$ - see front matter © 2004 Elsevier Ltd. All rights reserved.
doi:10.1016/j.ijheatmasstransfer.2004.05.014

Nomenclature

AR	aspect ratio
C_p	liquid specific heat
D	diameter of the propeller
Gr	Grashof number, $g\beta q'' D^4/(kv^2)$
H	height of the enclosure
k	liquid thermal conductivity
L	length of the heat source
Nu	local Nusselt number, $q''D/k\Delta T$
Pr	Prandtl number, v/α
q''	heat flux from the heat sources
Re	Reynolds number, $U_i D/v$
T	temperature
T_i	temperature at the right vertical wall
T_s	temperature at the heat sources
u	horizontal velocity component
U	dimensionless horizontal velocity component, u/U_i
U_i	velocity rate of the propeller
v	vertical velocity component
V	dimensionless vertical velocity component, v/U_i
x, y	Cartesian coordinates
X, Y	dimensionless Cartesian coordinates, $X = x/D,\ Y = y/D$

Greek symbols

β	coefficient of the thermal expansion
μ	absolute viscosity
v	kinematic viscosity
θ	dimensionless temperature, $k(T - T_i)/(q''D)$
ρ	density

enclosures. Several cases were performed and it was found that the interaction between heat sources and the separation between them play a key role in the development of the heat and fluid flow patterns.

A numerical and experimental analysis of a rectangular enclosure with four heat sources embedded on a vertical wall was done by Ho et al. [4]. The aspect ratio, location of the heat sources and the effect of Rayleigh number was investigated. Their results agreed with those obtained by Sezai and Mohamad [2] at different Rayleigh numbers. This study also shows that the convection flow of the air increases for high aspect ratios, forming multiple cells in the central region of the enclosure.

Combined forced and natural convection in enclosures and partial enclosures has also been investigated in the recent past. However, studies related to this subject were mainly concerned with vented enclosures. Calmidi and Mahajan [5] reported a numerical study of mixed convection on a heated horizontal surface within a partially open vertical enclosure using air as the working fluid. Two values of the Grashof number, 10^4 and 10^5, were considered for different Reynolds numbers, thus different ratios of Gr/Re^2 were calculated. They found that choosing the correct location for the exit boundary was crucial to the accuracy of the quantitative results.

Angirasa [6] presented a numerical study for mixed convection of airflow in an enclosure having an isothermal vertical wall. Forced conditions were imposed by providing an inlet and a vent in the enclosure. Both, positive and negative temperatures potentials were considered, making the Grashof number vary from -10^6 to 10^6. In their study steady-state solutions could not be obtained for higher positive values of the Grashof number and for buoyancy-dominated flows. In general, forced flow enhanced heat transfer for both negative and positive Grashof numbers.

Hsu and Wang [7] investigated the mixed convective heat transfer in an enclosure with heat sources embedded on a vertical board placed in the middle of the container. The heat sources were placed at different locations on the board and the enclosure had an inlet and a vent for the outgoing air. It was found that the arrangement of the dividing board in the enclosure generated significant changes in both the thermal flow field and the heat transfer coefficient.

Transient laminar mixed convection in a two-dimensional opened enclosure partitioned by a conducting baffle was numerically studied by How and Hsu [8]. The enclosure had a constant flux heat source of finite length, the inflow opening located on the left vertical wall and the outflow opening on the opposite wall. The study was performed for a range of Gr/Re^2 from 0.001 to 30. It was found that due to the interaction between the cold forced flow and the buoyancy-induced flow, the values of Nusselt number for all cases initially had a rapid decline, followed by a damping oscillation, and finally attaining steady state. It was also found that at lower values of Gr/Re^2, the Nusselt number appeared to increase only slightly with an increasing value of Gr/Re^2. This phenomenon indicated the fact that forced convection dominated the heat transport mechanism for small value of Gr.

Although air cooling continues to be the most widely used method for cooling electronic packages, it has long been recognized that significantly higher heat fluxes cannot be dissipated by this mean. The successful introduction of direct liquid immersion cooled super-

computers in the late 80s led to believe that the direct cooling with dielectric liquids may be the solution for computer chips in the very short-future. Tou et al. [9] performed a three-dimensional study of natural convection cooling of heat sources flush mounted on a vertical wall of a rectangular enclosure. The enclosure was filled with various liquids and cooled by the opposite wall. The results indicated that the flow field is complex since it is affected by the temperature field inside the enclosure.

The aim of this study is to investigate the forced convection imposed by a propeller in a closed, not-vented enclosure. The propeller is placed at two different locations of the enclosure. Within the enclosure three heat sources are embedded on a vertical wall, and the enclosure is filled with a dielectric fluid. Numerical solutions for the temperature and fluid fields are obtained for various Grashof numbers between 10^6 and 10^7, ratios of Gr/Re^2 between 0.2 and 2, and different aspect ratios of the enclosure.

2. Geometry model

The physical model and coordinate system of the problem under consideration are shown schematically in Fig. 1. Two cases are investigated for a two-dimensional-closed enclosure of height H and length C, filled with the dielectric fluid FC-70 manufactured by 3M. Three heat sources are flush-mounted on a vertical wall and provide a constant heat flux for both cases. The heat flux range for each of the three heat sources is varied between 10,000 and 100,000 W/m^2.

The dimensionless distances for each case of analysis are:

(a) *Case 1*. $D = E_1 = E_2 = 1$, $H = 7$, $S = 1.8$, $L = 1.4$, and C is varied from 2.8 to 7.
(b) *Case 2*. $D = 1$, $H = 7.2$, $S = 1.8$, $L = 1.4$, $E_1 = 1.8$, $E_2 = 0.4$, and C is varied from 3.6 to 7.2.

3. Governing equations

The mathematical description of the fluid flow and the convective heat transfer in the closed enclosure is based on a two-dimensional, incompressible, laminar flow, steady state formulation in a Cartesian coordinate system. The fluid properties are considered to vary with temperature. The compressible work and the viscous dissipation terms are neglected in the energy equation. The dimensionless equations describing the flow are as follows:

Continuity equation:

$$\frac{\partial U}{\partial X} + \frac{\partial V}{\partial Y} = 0 \tag{1}$$

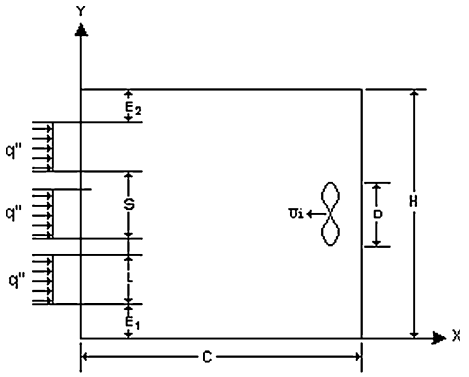

(a) Case 1.

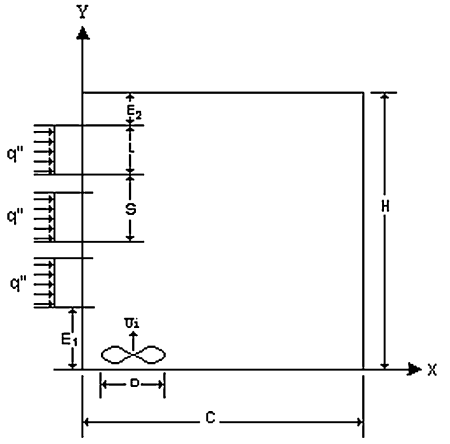

(b) Case 2.

Fig. 1. Geometry considered.

Momentum equations:

$$U\frac{\partial U}{\partial X} + V\frac{\partial U}{\partial Y} = -\frac{\partial P}{\partial X} + \frac{1}{Re}\left(\frac{\partial^2 U}{\partial X^2} + \frac{\partial^2 U}{\partial Y^2}\right)$$

$$U\frac{\partial V}{\partial X} + V\frac{\partial V}{\partial Y} = -\frac{\partial P}{\partial Y} + \frac{1}{Re}\left(\frac{\partial^2 V}{\partial X^2} + \frac{\partial^2 V}{\partial Y^2}\right) + \left(\frac{Gr}{Re^2}\right)\theta \tag{2}$$

Energy equation:

$$U\frac{\partial \theta}{\partial X} + V\frac{\partial \theta}{\partial Y} = \frac{1}{Pr\,Re}\left(\frac{\partial^2 \theta}{\partial X^2} + \frac{\partial^2 \theta}{\partial Y^2}\right) \tag{3}$$

The governing parameters that appear in the above equations are the Prandtl number, Pr; the Reynolds number, Re; and the buoyancy parameter Gr/Re^2, which describes the tendency of the phenomenon, whether it is natural convection, forced convection or mixed combined effects.

To compare the heat transfer characteristics of a system, the Nusselt number is usually employed. The

local heat transfer coefficient and Nusselt number on the heat source surface are calculated as:

$$h = \frac{q}{T_S - T_i} \tag{4}$$

$$Nu = \frac{hD}{k} \tag{5}$$

4. Boundary conditions

The boundary conditions for this analysis are:

(a) For the vertical wall where the heat sources are embedded ($X = 0$):

- At exactly the position where the heat sources are, the heat flux at the sources is given in a dimensionless fashion by:

$$\frac{\partial\theta}{\partial X} = -1 \tag{6}$$

- For the rest of the adiabatic wall:

$$\frac{\partial\theta}{\partial X} = 0 \tag{7}$$

- Non-slip flow condition at the wall

$$U = V = 0 \tag{8}$$

(b) For the rest of the walls:

- At $X = C/D$, the right-hand-side wall:

$$\theta = 0; \quad U = V = 0 \tag{9}$$

- At $Y = H/D$, the top of the enclosure:

$$\theta = 0; \quad U = V = 0 \tag{10}$$

- At the bottom, $Y = 0$:

$$\frac{\partial\theta}{\partial Y} = 0; \quad U = V = 0 \tag{11}$$

With the exception of the coefficient of thermal expansion, β, all properties for the fluid FC-70 vary with temperature, according to:

$$\rho(\mathrm{kg/m^3}) = 1984 - 1.93(T - 273) \tag{12}$$

$$k(\mathrm{W/mK}) = 0.07 - 0.00001(T - 273) \tag{13}$$

$$\mu(\mathrm{Pa \cdot s}) = (7\mathrm{E} + 20)T^{-9.0994} \tag{14}$$

$$C_p(\mathrm{J/kg\,K}) = 1014 + 1.554(T - 273) \tag{15}$$

where T must be given in Kelvin.

The coefficient of thermal expansion for the FC-70 fluid is:

$$\beta = 0.0010\,\mathrm{K^{-1}} \tag{16}$$

Values of fluid properties were provided by 3M [10].

Forced flow conditions are imposed by a propeller operated by an external motor with a nominal power of 5.61 W. Small propellers of this type have a typical uniform flow of about 2 m/s, however for implementing the effects of the propeller in the fluid domain, the pressure rise associated with it is considered. The pressure gradient as a function of velocity is given by:

$$\frac{\partial p}{\partial s} = 6.7861u_i + 562715 \tag{17}$$

where s is an arbitrary direction in the Cartesian coordinates and u_i is the velocity for the s-direction, and obtained from data for typical propellers of this size.

5. Numerical analysis

According to the position of the propeller, two cases were investigated, described as follows:

(a) *Case 1*. Propeller centered on the enclosure next to the right-hand-side vertical wall facing the heat sources. For this case the value of the aspect ratio (AR) is kept constant as 2.5, 1.81, 1.43, 1.18, 1, respectively, while the ratio Gr/Re^2 varies.

(b) *Case 2*. Propeller placed next to the left wall underneath the heat sources. For this case the value of AR is kept as 1.8, 1.5, 1.2, 1, and, as in Case 1, the ratio Gr/Re^2 varies.

Numerical solutions for the governing equations with the associated boundary conditions were obtained using finite element techniques. The numerical simulations were performed varying the number of elements of the grid in order to increase the accuracy and efficiency for the solutions. Non-uniform grids were employed in the analysis, with denser grids clustering in regions near the heat sources and the enclosed walls. The pressure gradient due to the propeller is a condition of momentum imposed exactly where the propeller is situated (along its diameter), modeling the effect that the propeller has on the fluid next to it.

6. Results

The heat sources considered in this study provide constant heat fluxes varying from 10,000 to 100,000 W/m^2, which are the typical heat fluxes of current computer chips, such as Pentium IV which provides a heat flux of about 60,000 W/m^2 [11]. This heat flux range corresponds to a ratio Gr/Re^2 between 0.2 and 2. The ratio Gr/Re^2 was obtained varying the Grashof number for each aspect ratio considered, whereas the Reynolds number was maintained as a constant for all cases.

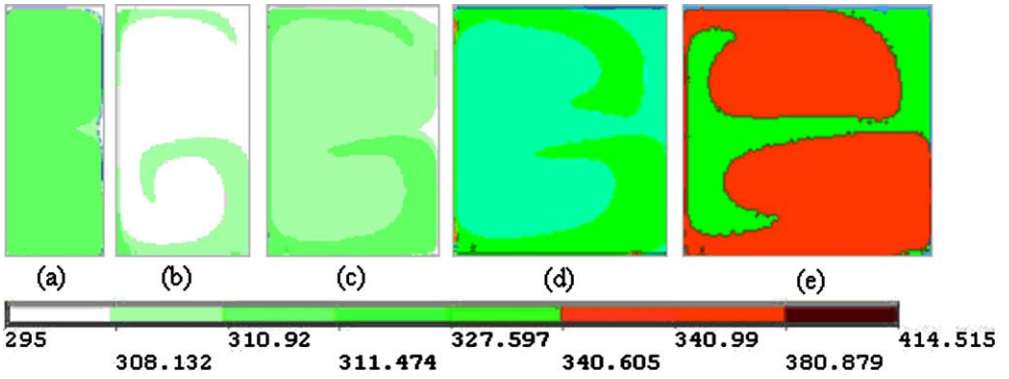

Fig. 2. Temperature fields for different aspect ratios and $Gr = 3.8 \times 10^7$. Case 1: (a) AR = 2.5, (b) AR = 1.81, (c) AR = 1.43, (d) AR = 1.18, and (e) AR = 1.

Case 1. Fig. 2 shows the temperature fields for the different aspect ratios, a heat flux of 100,000 W/m^2 and a ratio $Gr/Re^2 = 2$, therefore expecting natural convection to play a role in the energy dissipation. The propeller was placed near the vertical wall opposite to the wall where the heat sources were embedded; a dimensionless separation of about 0.98 between the wall and the propeller was considered. Since this separation between the vertical wall and the propeller is kept as constant, it can be observed that as the aspect ratio increases the forced fluid flow is much stronger near the region where the heat sources are placed. It was found that the maximum temperature occurs above the top of the highest heat source for all aspect ratios considered, whereas the central region of the enclosure has the lowest temperature due to the forced fluid conditions provided by the propeller. Another hot point is located near the bottom left corner of the enclosure. The results show that this configuration allows to keep the largest temperature away from the heat sources, avoiding an increase in the chips temperature.

The variation of the maximum temperature in terms of the aspect ratio is shown in Fig. 3. It is clearly seen that the maximum temperature decreases as the aspect ratio increases within the region where AR < 1.43, beyond which the maximum temperature is nearly constant as the aspect ratio increases. This implies that the minimal temperature distribution may occur at an aspect ratio of 1.43. The minimal temperature is of importance to achieve the optimal heat transfer effect inside the enclosure since it cannot be simply stated that the larger or the smaller the aspect ratio, the lower the temperature.

Fig. 4 shows the dimensionless temperature at the vertical wall where the heat sources are embedded. It is clearly seen that the temperature decreases as the distance increases for $Y < 2.5$, and remains more or less constant within the region where $2.5 < Y < 4.5$, whereas

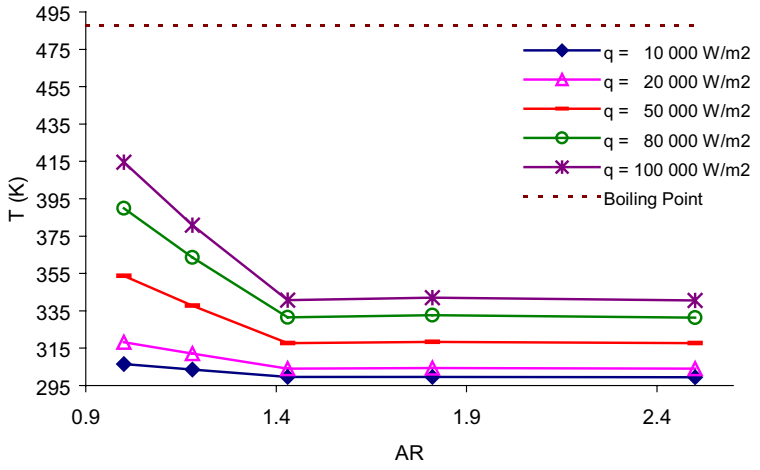

Fig. 3. Effects of the aspect ratio on the maximum temperature for Case 1.

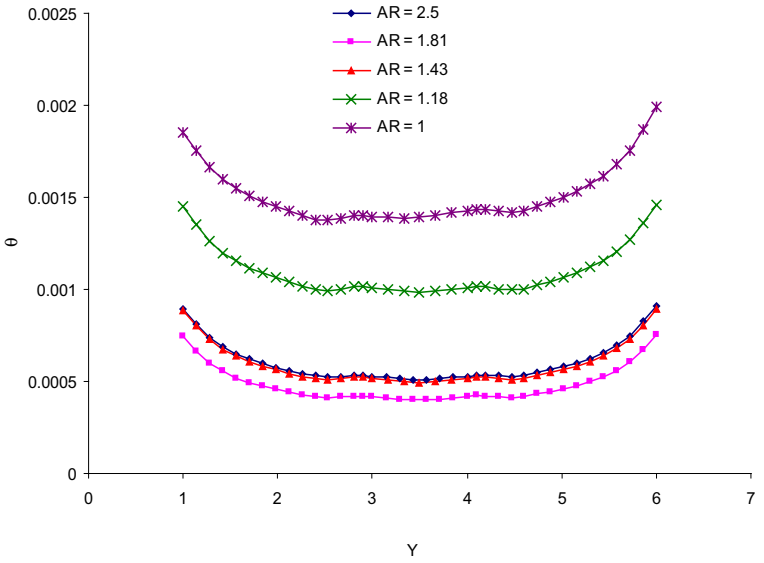

Fig. 4. Dimensionless temperature at the vertical wall where the heat sources are placed, Case 1.

temperature increases as the distances increases for $Y > 4.5$. Thus, the lowest temperature is found in the central heat source, as expected. Although the variation of temperature looks symmetrical for $Y = 3.5$, the maximum temperature was reached above the highest heat source ($Y = 6$) and it was slightly larger than the temperature at the lowest heat source, which indicates that natural convection plays a role in the effective heat transfer. It is evident from Fig. 4 that forced convection is predominant in this analysis and therefore, the asymmetry for $Y = 3.5$ is hardly detectable.

The local Nusselt number along the Y distance is plotted in Fig. 5. Results show, as expected, that the local Nusselt number increases as the Y distance increases for $Y < 3.5$; at $Y = 3.5$ (central heat source) the Nusselt number reaches its higher value and for $Y > 3.5$ the Nusselt number decreases as the Y distance increases. It is clearly seen that the Nusselt number increases as the aspect ratio increases within the region where $AR < 1.81$; when $AR > 1.81$ the Nusselt number becomes smaller. This can readily be explained because as the aspect ratio increases the amount of dielectric fluid working as a coolant is smaller.

The fluid behavior for all aspect ratios considered is shown in Fig. 6. As it was expected, the fluid travels along the enclosure from the propeller placed next to the right-hand-side wall to the opposite wall where the heat sources are placed and splits at this point forming two rotating cells and generating a stagnation region at the central heat source. Other stagnation regions can be observed at the corners of the enclosure and it was found that as the aspect ratio decreases the stagnation regions become larger. It is clearly seen that the forced fluid flow is much stronger in the region where the heat sources are placed as the aspect ratio increases. As the aspect ratio approaches 1, the fluid flow near the heat sources is weaker and the two rotating cells become a bit asymmetric due to the effect of natural convection. It was found that both, the temperature fields and the fluid behavior, were similar for all cases of the heat flux range considered.

Case 2. Fig. 7 presents the temperature field for Case 2, with a constant heat flux of 20,000 W/m^2, and a ratio $Gr/Re^2 = 0.419$. Although Case 2 was performed for the whole heat flux range described earlier, it was found that the dielectric fluid reached its boiling point for high heat fluxes and $AR > 1.2$. In order to draw some valuable comparisons and conclusions for this case, it was decided to present results for low values of heat flux and Gr/Re^2 ratios. The propeller was placed underneath the heat sources (sending the forced flow in a way parallel to the heat sources) and it was kept in the same position for all aspect ratios. It can be inferred that this is the best position for the propeller since forced fluid conditions are added to the effects of natural convection therefore increasing the effective heat transfer. It can be observed from Fig. 7 that maximum temperatures within the enclosure occur at the region where the top heat source is placed, whereas the rest of the fluid within enclosure has almost a uniform temperature, except for $AR = 1$.

Fig. 8 shows the variation of the maximum temperature within the enclosure in terms of the aspect ratio. It is clearly seen that as the aspect ratio increases from 1 to 1.2 the maximum temperature decreases, and from this point on, as the aspect ratio increases the maximum temperature increases. It can also be observed from

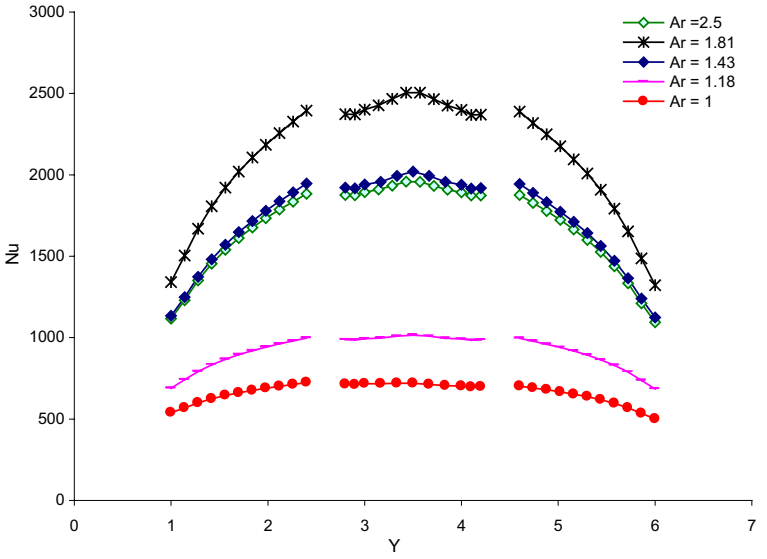

Fig. 5. Local Nusselt number at the heat sources, Case 1.

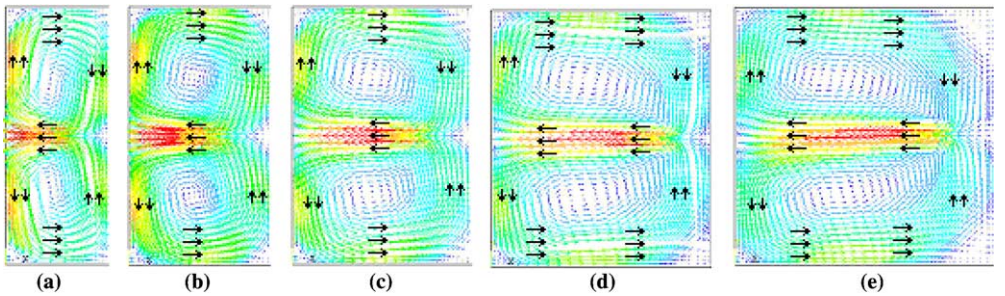

Fig. 6. Velocity vectors for different aspect ratios and $Gr = 3.8 \times 10^7$. Case 1: (a) AR = 2.5, (b) AR = 1.81, (c) AR = 1.43, (d) AR = 1.18 and (e) AR = 1.

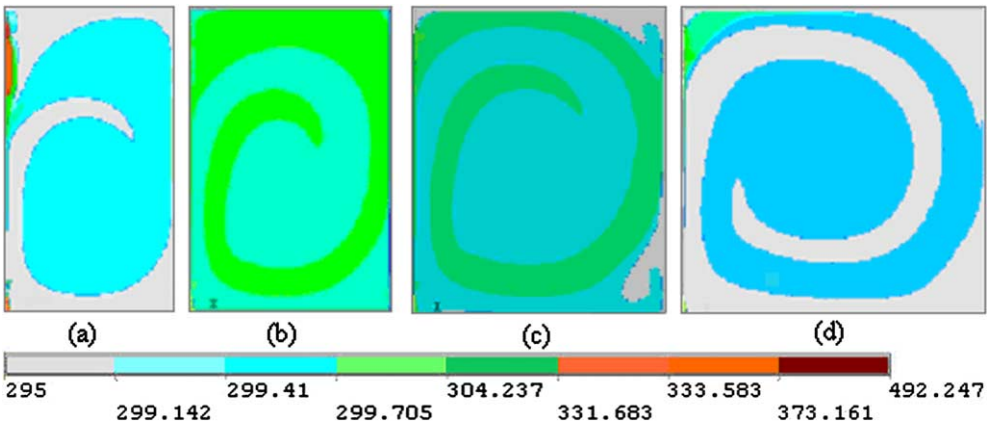

Fig. 7. Temperature fields for different aspect ratios and $Gr = 7.6 \times 10^6$. Case 2: (a) AR = 1.8, (b) AR = 1.5, (c) AR = 1.2, (d) AR = 1.

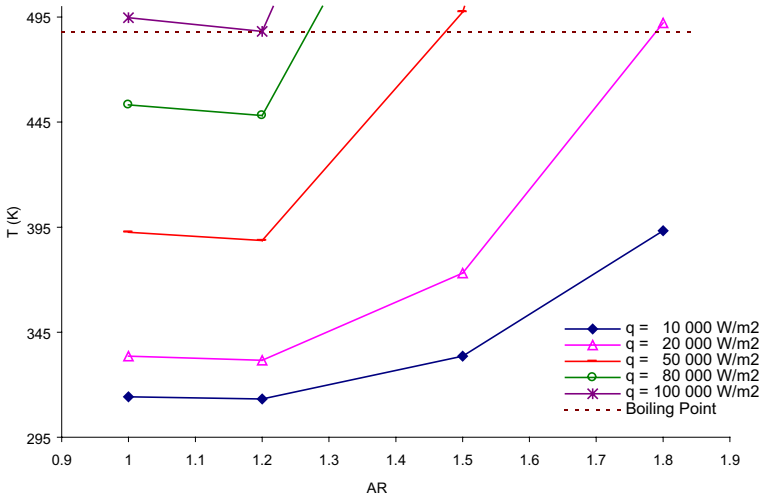

Fig. 8. Effects of the aspect ratio on the maximum temperature for Case 2.

Fig. 8 that the boiling point of the fluid is reached when heat fluxes of about 100,000 W/m^2 are considered, for all aspect ratios. Likewise, as AR > 1.2 the dielectric fluid reaches its boiling point for heat fluxes larger than 20,000 W/m^2. Therefore, an aspect ratio of 1.2 should be considered as the better option for this configuration since it allows to keep the lowest maximum temperature of the heat flux range considered without reaching the boiling point of the fluid.

Fig. 9 shows the dimensionless temperature (semi-algorithmic scale is used in order to appreciate the tendency) along the vertical wall where the heat sources are embedded. As the Y distance increases the dimensionless temperature increases very slightly within the region where $Y < 5$, which corresponds to the place where the lowest and central heat sources are located, this means that forced convection in this region is very strong.

When $Y > 5$ (highest heat source) two different tendencies can be observed for the different aspect ratios considered: (1) for $1 < AR < 1.5$ it was found that the dimensionless temperatures increases as the Y distance increases from $Y = 5$ to 6 (central part of the top heat source), and from this point forward the dimensionless temperature starts a decrease due to the closeness to the top wall of the enclosure which is maintained at a constant temperature; (2) for AR = 1.8 it was found that the dimensionless temperature increases rapidly as the Y distance increases. Although the top wall is at the same

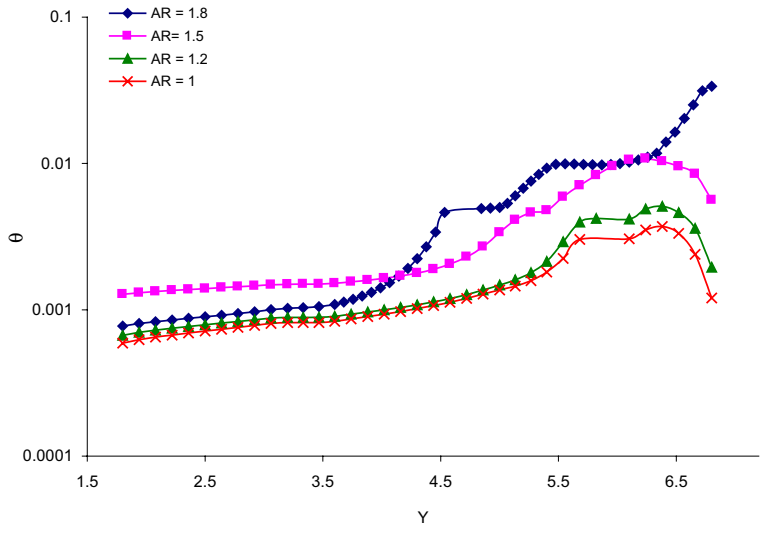

Fig. 9. Dimensionless temperature at the vertical wall where the heat sources are placed, Case 2.

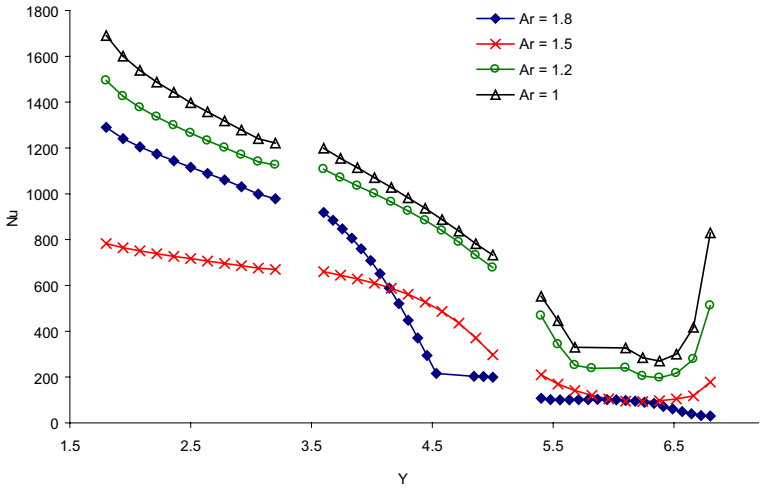

Fig. 10. Local Nusselt number at the heat sources, Case 2.

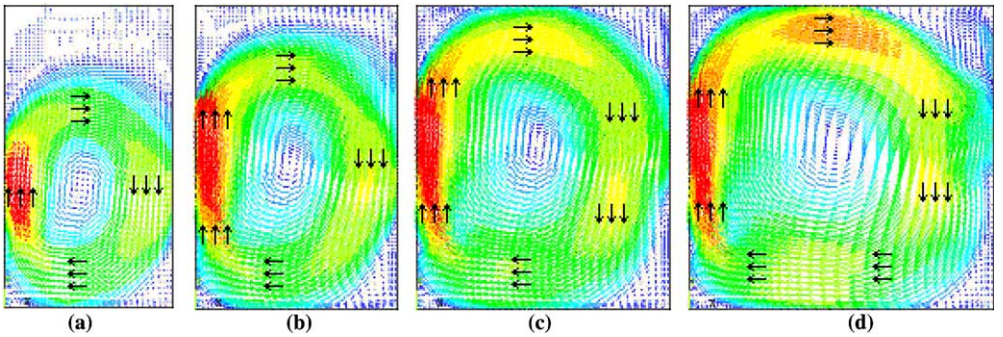

Fig. 11. Velocity vectors for different aspect ratios and $Gr = 7.6 \times 10^6$. Case 2. (a) AR = 1.8, (b) AR = 1.5, (c) AR = 1.2, (d) AR = 1.

distance for all aspect ratios, it was found that for AR = 1.8 the forced fluid flow in the top heat source region is almost neglected, causing an increase of temperature within this region. This will be explained further in Fig. 11.

The local Nusselt number variation at the surface of the heat sources is plotted in Fig. 10. It is seen that the maximum Nusselt number is found at $Y = 2$ (the beginning of the lowest heat source) where the thermal boundary layer begins to develop. Forced fluid flow gets hotter as it flows upwards along the vertical wall, therefore decreasing the Nusselt number. However, after its decreasing tendency, the Nusselt number increases rapidly as it approaches the edge of the top heat source for AR = 1 and 1.2, whereas for AR = 1.5 the Nusselt number increases only very slightly and for AR = 1.8 it keeps its decreasing tendency. The abrupt increase in the Nusselt number can be explained in the following way: near the region where $Y = 7$ the thermal boundary layer is probably already separated and, at the same time there is a small counter-clockwise recirculation at the top left corner of the enclosure with fluid flow near to the vertical wall giving as a result the formation of a second boundary layer around $Y = 7$.

The fluid behavior, having a single rotating cell developing, is shown in Fig. 11 for Case 2. Since there was a dimensionless separation of 0.2 between the propeller and the vertical wall where the heat sources are embedded, a small stagnation area can be seen in this region, although not affecting the general results of the analysis. The results show that for AR = 1 and 1.2 the rotating cell develops occupying the whole space within the enclosure (except for the corners), whereas when the aspect ratio increases the rotating cell tries to keep its circular form not reaching the top wall of the enclosure.

Stagnation regions are observed at the corners of the enclosure and at the highest part of the enclosure for AR = 1.5 and 1.8, which indicates that the fluid at these regions is not doing its job as a coolant, but develops somehow stagnant. This suggests that the geometry of

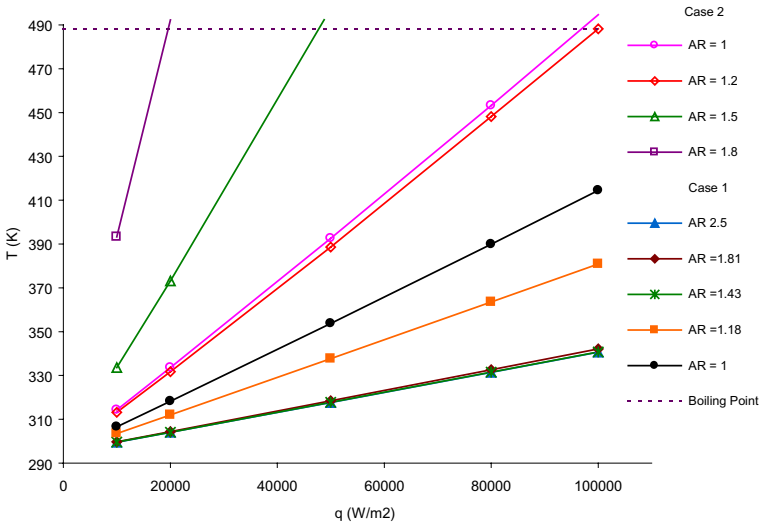

Fig. 12. Maximum temperature within the enclosure for both Cases.

the enclosure could be changed by smoothing out the corner areas, aiding the circulation of the fluid. It is remarkable that the temperature and fluid fields were similar for all cases of heat flux range considered in the analysis.

Fig. 12 shows the variation of maximum temperature reached by the fluid for the heat flux range considered in this analysis, for both cases. The largest temperatures for all aspect ratios for Case 1 and for AR = 1 and 1.2 for Case 2, do not reach the boiling point of the fluid (488 K) for the whole heat flux range considered in the analysis. It is interesting that this does not happen, since in an earlier study by Grimaldi et al. [12], it was found that for smaller heat fluxes of the heat sources the boiling point of the same dielectric fluid (FC-70) was reached, making the cooling process not feasible by means of natural convection alone (that study was performed for natural-cooling means only). In the present study it was found that the boiling point of the dielectric fluid is reached for heat fluxes larger than 20,000 W/m^2 when AR $\geqslant$ 1.5 only for Case 2.

7. Conclusions

The effects of coupled forced-convective-flow and natural-convective-flow cooling in a completely closed enclosure filled with dielectric fluid have been investigated. Fluid patterns were found for two different cooling schemes, Case 1 having the cooling propeller facing the intensive-high-sources, and Case 2 having the cooling propeller underneath the sources (and sending the forced flow in a way parallel to the wall where the heat sources are located). Three heat sources, each having a heat flux in the ranges of 10,000–100,000 W/m^2, were placed on a vertical wall of the enclosure.

Results showed that the top heat source was in all cases the hottest source. From the temperature and velocity fields for both cases, it can be inferred that Case 1 could provide the best cooling for the heat sources, since energy is distributed throughout a larger region making the upper left corner of the enclosure be the region where the maximum temperatures are reached, whereas in Case 2, the largest temperatures occurred right by the heat sources, not dissipating as well the energy. It can be also seen that Case 1 provides the best cooling option for the heat sources since the dielectric fluid does not reach its boiling point for any aspect ratios considered in this analysis, whereas in Case 2, the dielectric fluid reaches its boiling point for AR $\geqslant$ 1.5.

Although the propeller for Case 2 was placed in such a way that the forced fluid flows parallel to the heat sources (aiding natural convection), convective heat transfer is much larger for Case 1 due to the fact that the forced fluid flow hits the heat sources in a perpendicular direction. Therefore, it can be concluded that the location of the propeller for Case 1 makes the effective heat transfer removal more efficient.

The fact that the boiling point of the dielectric liquid is not reached for all aspect ratios for Case 1 and for several aspect ratios for Case 2, even when highly-intensive heat fluxes are placed, implies that mixed convection cooling (forced plus natural convection), using a dielectric liquid as the working fluid, may become the solution of cooling for computer chips in the very short future.

References

[1] P. Tadayon, Thermal challenges during microprocessor testing, in: Intel Technol. J., Q3, 2000. Available from <www.intel.com>.

[2] I. Sezai, A.A. Mohamad, Natural convection from discrete heat source on the bottom of a horizontal enclosure, Int. J. Heat Mass Transfer 43 (2000) 2257–2266.

[3] Q.H. Deng, G.F. Tang, Y. Li, M.Y. Ha, Interaction between discrete heat sources in horizontal natural convection enclosures, Int. J. Heat Mass Transfer 45 (2002) 5117–5132.

[4] C.J. Ho, J.Y. Chang, A study of natural convection heat transfer in a vertical rectangular enclosure with two-dimensional discrete heating: effect of aspect ratio, Int. J. Heat Mass Transfer 37 (6) (1994) 917–925.

[5] V.V. Calmidi, R.L. Mahajan, Mixed convection over a heated horizontal surface in a partial enclosure, Int. J. Heat Fluid Flow 19 (1998) 358–367.

[6] D. Angirasa, Mixed convection in a vented enclosure with an isothermal vertical surface, Fluid Dynam. Res. 26 (2000) 219–223.

[7] T.H. Hsu, S.G. Wang, Mixed convection in a rectangular enclosure with discrete heat sources, Num. Heat Transfer, Part A 38 (2000) 627–652.

[8] S.P. How, T.H. Hsu, Transient mixed convection in a partially divided enclosure, Comput. Math. Appl. 36 (8) (1998) 95–115.

[9] S.K.W. Tou, C.P. Tso, X. Zhang, 3D Numerical analysis of natural convective liquid cooling of a 3×3 heater array in rectangular enclosures, Int. J. Heat Mass Transfer 42 (1999) 3231–3244.

[10] 3M Fluorinert™ Electronic Liquid FC-70, Product Information, Issued: 05/00, www.3m.com, 2000, pp. 1–2.

[11] Intel® Pentium® 4 Processor in the 478-Pin Package Thermal Design Guidelines, available from: www.intel.com, May 2002, p. 13, 27.

[12] A. Fuentes-Grimaldi, A. Hernandez-Guerrero, R. Lesso-Arroyo, R. Romero-Mendez, Study on the necessary flow rates for the cooling of high energy sources within an enclosure filled with dielectric fluid, in: Proceedings of the 6th ASME-JSME Thermal Engineering Joint Conference, March 16–20, Hawaii, USA, 2003.